Published in final edited form as:
Ophthalmology. 2014 January ; 121(1): 162–172. doi:10.1016/j.ophtha.2013.07.013.

Quantitative Classification of Eyes with and without Intermediate Age-related Macular Degeneration Using Optical Coherence Tomography

Sina Farsiu, PhD[1,2,3], **Stephanie J. Chiu, BS**[2], **Rachelle V. O'Connell, BS**[1], **Francisco A. Folgar, MD**[1], **Eric Yuan, BS**[1], **Joseph A. Izatt, PhD**[1,2], **Cynthia A. Toth, MD**[1,2], and **the Age-Related Eye Disease Study 2 Ancillary Spectral Domain Optical Coherence Tomography Study Group**[*]

[1] Department of Ophthalmology, Duke University Medical Center, Durham, North Carolina.

[2] Department of Biomedical Engineering, Duke University, Durham, North Carolina.

[3] Department of Electrical & Computer Engineering, Duke University, Durham, North Carolina.

Abstract

Objective—To define quantitative indicators for the presence of intermediate age-related macular degeneration (AMD) via spectral-domain optical coherence tomography (SD-OCT) imaging of older adults.

Design—Evaluation of diagnostic test and technology.

Participants and Controls—One eye from 115 elderly subjects without AMD and 269 subjects with intermediate AMD from the Age-Related Eye Disease Study 2 (AREDS2) Ancillary SD-OCT Study.

Methods—We semiautomatically delineated the retinal pigment epithelium (RPE) and RPE drusen complex (RPEDC, the axial distance from the apex of the drusen and RPE layer to Bruch's membrane) and total retina (TR, the axial distance between the inner limiting and Bruch's membranes) boundaries. We registered and averaged the thickness maps from control subjects to generate a map of “normal” non-AMD thickness. We considered RPEDC thicknesses larger or smaller than 3 standard deviations from the mean as abnormal, indicating drusen or geographic atrophy (GA), respectively. We measured TR volumes, RPEDC volumes, and abnormal RPEDC thickening and thinning volumes for each subject. By using different combinations of these 4 disease indicators, we designed 5 automated classifiers for the presence of AMD on the basis of the generalized linear model regression framework. We trained and evaluated the performance of these classifiers using the leave-one-out method.

Correspondence: Sina Farsiu, PhD, Box 3802, DUMC, Durham, NC 27710. sina.farsiu@duke.edu..

[*]A full listing of the AREDS2 Ancillary SD-OCT Study Group is available at http://aaojournal.org.

Presented at: the American Academy of Ophthalmology Annual Meeting, November 10e13, 2012, Chicago, Illinois.

Financial Disclosure(s):
The author(s) have made the following disclosure(s): S.F. and S.J.C.: Duke University (patents/royalty). R.V.O., F.A.F., and E.Y.: none. J.A.I.: Duke University (patents/royalty); Bioptigen, Inc. (personal financial interest, patent, nonremunerative). C.A.T.: Duke University (patents/royalty), Alcon (patents/royalty), Genentech (research), Bioptigen (research), Physical Sciences Inc (research). Dr. Izatt is co-founder and Chief Science Advisor for Bioptigen, Inc. and has corporate, equity, and intellectual property interests (including royalties) in this company. Duke University also has equity and intellectual property interests (including royalties) in Bioptigen, Inc.

Main Outcome Measures—The range and topographic distribution of the RPEDC and TR thicknesses in a 5-mm diameter cylinder centered at the fovea.

Results—The most efficient method for separating AMD and control eyes required all 4 disease indicators. The area under the curve (AUC) of the receiver operating characteristic (ROC) for this classifier was >0.99. Overall neurosensory retinal thickening in eyes with AMD versus control eyes in our study contrasts with previous smaller studies.

Conclusions—We identified and validated efficient biometrics to distinguish AMD from normal eyes by analyzing the topographic distribution of normal and abnormal RPEDC thicknesses across a large atlas of eyes. We created an online atlas to share the 38 400 SD-OCT images in this study, their corresponding segmentations, and quantitative measurements.

Financial Disclosure(s)—Proprietary or commercial disclosure may be found after the references.

Age-related macular degeneration (AMD) is the leading cause of irreversible blindness in elderly Americans.[1] To investigate the location and pattern of microanatomic retinal and subretinal changes early in the disease process, several large-scale longitudinal studies using in vivo spectral-domain optical coherence tomography (SD-OCT) are under way. In comparison with the classic en face color fundus photograph, the cross-sectional view of the retina from SD-OCT should better characterize the vitreoretinal interface, retina, geographic atrophy (GA), retinal pigment epithelium (RPE), and drusen in eyes with non-neovascular AMD.[2–4] Drusen area and pigmentary abnormalities as seen on color fundus photographs are measures of disease severity and predict the likelihood of progression to advanced AMD.[5–8] In SD-OCT, AMD disease severity is likely to be determined from quantification of drusen[3,9,10] and GA.[11,12] Although eyes with later stages of intermediate AMD containing excess drusen or non-central GA are easy to distinguish from normal eyes, it is time-consuming to review multiple scans to identify distinguishing features especially when they are sparse and minimal as in early disease. This is primarily due to the gradual changes of the RPE toward GA (an abnormally thin RPE) or drusen (an abnormally thick RPE).

There have been several excellent reports on the average retinal layer thicknesses (including the RPE) for different retinal diseases measured on SD-OCT images,[13–15] and Pappuru et al[16] correlated outer retinal layer thicknesses and visual acuity in 100 eyes with non-neovascular AMD. Our prospective study on 384 subjects is by far the largest quantitative SD-OCT study conducted on RPE thickness and its abnormalities. In this article, we sought efficient biometrics to detect eyes with intermediate non-neovascular AMD as seen on SD-OCT and differentiate them from elderly control eyes, using the dataset from the Age-Related Eye Disease Study 2 (AREDS2) Ancillary SD-OCT (A2A SD-OCT) Study. This prospective, multicenter, multi-year, randomized trial is designed to determine whether early AMD features quantified on SD-OCT can be used to predict vision loss and progression to advanced disease. We sought the normal range and topography for retinal and RPE measurements in both groups to relate findings from this study to measurements used in previous AMD studies[17] and large-scale clinical trials.[18,19] The main goals of our article are to demonstrate the location-specific normal range and distribution of the RPE and RPE drusen complex (RPEDC, the axial distance from the apex of the drusen and RPE layer to Bruch's membrane) and total retina (TR, the axial distance between the inner limiting and Bruch's membranes) thicknesses within a 5-mm circle centered at the fovea and to demonstrate the effectiveness of a novel method that uses these maps to distinguish normal eyes from those with intermediate AMD.

Methods

Dataset

For this study, we used the dataset from the A2A SD-OCT Study, which was registered at ClinicalTrials.gov (Identifier: NCT00734487) and approved by the institutional review boards of the 4 A2A SD-OCT clinics (Devers Eye Institute, Duke Eye Center, Emory Eye Center, and National Eye Institute). With adherence to the tenets of the Declaration of Helsinki, informed consent was obtained from all subjects.

The AREDS2 and A2A SD-OCT Study design and protocol for grading fundus photographs (AREDS2) and SD-OCT images (A2A SD-OCT) have been described.[20,21] In brief, subjects who met the following inclusion criteria were enrolled: between 50 and 85 years of age, exhibiting intermediate AMD with large drusen (>125 μm) in both eyes or large drusen in 1 eligible eye and advanced AMD in the fellow eye, with no history of vitreoretinal surgery or ophthalmologic disease that might affect acuity in either eye. Age-appropriate control subjects were enrolled with the same inclusion criteria as for AREDS2 except that they must have had no evidence of macular drusen or AMD in either eye at the baseline visit or in the follow-up years. Stereoscopic color fundus photograph pairs were taken at the baseline visit as part of the AREDS2 protocol[20] and then graded by certified readers at the Wisconsin Fundus Photography Reading Center (University of Wisconsin, Madison, WI). For our study, eyes assigned a Wisconsin drusen area score of “cannot grade” (drusen area was only partially visible for the field under consideration, such as when an obscuring lesion or poor photographic quality did not permit a reasonably confident assessment of drusen) at the Wisconsin Center were excluded.

The SD-OCT imaging systems from Bioptigen, Inc (Research Triangle Park, NC), located at the 4 clinic sites, were used to acquire volumetric rectangular (~6.7 × ~6.7 mm) scans as previously published.[21] To summarize, for all subjects, 0° and 90° rectangular volumes centered at the fovea (defined as volumes acquired with the fast scan direction oriented horizontally and vertically, respectively) with 1000 A-scans per B-scan and 100 B-scans per volume were captured for both eyes. In the A2A SD-OCT Study, of the 345 participants with AMD, 314 had at least 1 eye with intermediate AMD, and of the 122 control subjects without AMD, 119 had no eye disease at baseline.[21] From these, 1 eligible eye of each subject had been randomly selected as the study eye as detailed by Leuschen et al.[21] Eye length was not measured. Certified SD-OCT readers assessed the scan quality for each volume.[21] For this study, we selected the 0° volumes by default, and any poor-quality (as assessed by graders) 0° volumes were replaced by a 90° volume from the same visit; if both scan volumes were poor, then the eye was excluded altogether. The excluded eyes were mainly those that contained blank or extremely low-quality images due to blinks or imaging errors or those volumes that exhibited significant eye motion or loss of fixation during image acquisition. Thus, in this study, we analyzed 269 of the 314 eyes with intermediate AMD and 115 of the 119 control (normal) eyes.

Quantitative Measurements

We isolated the RPEDC according to its definition and marking guidelines outlined in our previous publication.[22] This was accomplished by delineating the inner aspect of the RPE plus drusen material and the outer aspect of Bruch's membrane. Thus, for macular SD-OCT datasets with non-neovascular AMD, the RPEDC volume contained all drusen material (including subretinal drusenoid deposits), whether above or below the RPE, and contained all RPE material, whether normal or atrophied (an indicator of GA).

We also delineated the inner aspect of the inner limiting membrane (ILM) to obtain the TR volume (between the ILM and the inner aspect of Bruch's membrane) and neurosensory retinal (NSR, from the ILM to the inner aspect of RPEDC) (Fig 1) volume.

Analysis Software

We imported all images into a custom program, the Duke OCT Retinal Analysis Program (DOCTRAP), based in MATLAB (The MathWorks Inc, Natick, MA). The core algorithm of this software is based on the generalized graph theory and dynamic programming framework.[23] DOCTRAP has the capability to automatically delineate retinal layer boundaries for normal, AMD, and diabetic eyes[22,23] in SD-OCT images. It also features a graphical user interface (GUI) that allows for the manual correction of possible errors in the automatic segmentation. We performed all other routine image processing and statistical analysis processes using native functions in MATLAB.

Image Analysis Process

We delineated the boundaries of the RPEDC and TR regions for all eyes in 2 steps. First, we used DOCTRAP (version 14.1.2) to automatically segment the target retinal layer boundaries in both the normal patients and patients with AMD.[22] Second, all SD-OCT images were reviewed for possible manual correction after automated segmentation. We used DOCTRAP's GUI for manual correction of possible segmentation errors by graders certified by the Duke Advanced Research in Spectral Domain OCT Imaging laboratory, and the location of the fovea was manually marked on its corresponding B-scan using a separate GUI feature. The SD-OCT graders did not know which eyes were designated as AMD or control on the basis of color fundus examination. We then used the accurate layer boundary positions to generate RPEDC and TR thickness maps 100 × 1000 pixels in size and interpolated these maps to 1001 × 1001 pixels to achieve equivalent resolutions in both en face (X-Y) directions. Thickness values were converted from pixels to microns according to axial resolutions specified in Table 1 of our recent publication.[22]

Next, we rotated all 384 thickness maps such that they were oriented with the superior retina on top and the nasal retina to the right. Thickness maps were then registered (aligned) according to the fovea. We limited our analysis to a 5-mm diameter cylinder centered at the fovea to exclude parapapillary atrophy from the analysis and to avoid eliminating eyes from the study because of “partial maps.” Representative thickness maps for control subjects and subjects with AMD are illustrated in Figure 2.

For control and AMD eyes, we generated mean and standard deviation thickness maps for the RPEDC (controls, Fig 3A, B; AMD, Fig 3C, D) and TR (controls, Fig 4A, B; AMD, Fig 4C, D, available at http://aaojournal.org). We created control upper and lower limit thickness maps for the RPEDC (Fig 3E, F) and TR (Fig 4E, F, available at http://aaojournal.org) that represent the bounds for “normal” RPEDC or TR thickness. The control upper limit map was generated by adding 3 control standard deviation maps to a control mean map, and the control lower limit map was generated by subtracting 3 control standard deviation maps from a control mean map. For all thickness maps, we deemed thicknesses outside 3 control standard deviations from the control mean as abnormally thick or thin, that is, indicative of drusen or GA, respectively. We calculated an *abnormal thickness score* (μm^3) for each eye by (1) creating a difference map, defined as the individual thickness map subtracted by the control upper limit map; (2) setting all negative difference values to zero; and (3) summing all values on the difference map. We repeated these steps to generate an *abnormal thinness score* (μm^3) for each eye, with the difference map defined as the control lower limit map subtracted from the individual thickness map. These abnormality scores correspond to the total volumes of excess thickness and thinness, respectively.

Statistical Analysis

We used the abnormality scores to blindly classify the eyes from our dataset into subjects with AMD and control subjects. Our automated classifier was based on the generalized linear model regression,[24] as implemented by the MATLAB function *glmfit.m*, considering the binomial distribution in the learning phase and logistic regression parameters for the evaluation phase. We relied on the "leave-one-out" approach (a special case of the cross-validation method) to optimally use our dataset.[25] That is, we left 1 of the 384 eyes out of our training dataset and used this eye to validate the classification performance. We iterated this approach for all eyes in the dataset to not bias our estimated classification performance with respect to any particular datum.

We compared the performance of 5 different methods: method 1, classifying eyes using only TR volume as the predicting element for each eye; method 2, using only RPEDC volume; method 3, using only the abnormal RPEDC thickness score; method 4, using abnormal RPEDC thickness and thinness scores as the elements of a [2 × 1] prediction vector for each eye; and method 5, using TR and RPEDC volumes and abnormal RPEDC thickness and thinness scores as the elements of a [4 × 1] prediction vector for each eye. We generated the receiver operating characteristic (ROC) curve[26] for each classification method and used the area under curve (AUC) of the ROC to compare classification performances.[27] To obtain the best classification results for each method, the prediction vector biomarkers (e.g., RPEDC thickness, thinness score) were calculated on the basis of a set of cylinders with diameters between 0.2 and 5 mm with step size of 0.1 mm centered at the fovea. For each method, we chose the prediction vectors from the cylinder diameter that produced the highest AUC value.

Results

Comparison of Thickness Maps in Control Subjects and Subjects with Age-Related Macular Degeneration

The age range of the normal subjects was 51 to 83 years (mean, 66.6 years), and the age range of the subjects with AMD was 51 to 87 years (mean, 74.6 years). Figure 5 shows the mean and standard deviation of the TR and RPEDC thicknesses as a function of the distance from the fovea. For control subjects, the RPEDC and TR were thickest at 0.5 mm (33.0±4.3 μm thickness) and 1.00 mm (317.0±19.3 μm) distances from the fovea, respectively. Of note, the control eyes exhibited a statistical difference when comparing the RPEDC thickness at the fovea (30.7±5.7 μm) with the maximum RPEDC thickness (Wilcoxon rank-sum test, $P < 0.0001$). For subjects with AMD, the RPEDC thickness was maximum at the fovea (56.3±48.4 μm) and decreased monotonically as a function of distance from the fovea. Also in AMD eyes, the TR was at a 0.97 mm maximum distance from the fovea (329.5±33.7 μm). The RPEDC and TR thicknesses were on average significantly higher in the AMD eyes compared with control eyes (e.g., RPEDC thickness was 35.08±11.8 μm in AMD eyes vs. 28.3±3.8 μm in control eyes at 1.5 mm away from the fovea, Wilcoxon rank-sum test, $P < 0.0001$).

However, the AMD and control thicknesses are largely overlapping for both the RPEDC and TR (Fig 5). To better justify this claim, the histograms in Figure 6 (available at http://aaojournal.org) show that (unlike other biomarkers) a simple thresholding of abnormal RPEDC thickness score could correctly separate most subjects into the control and AMD groups.

Figure 7 shows probability maps of abnormal thickening and thinning for the TR and RPEDC in control and AMD eyes. For example, a probability of 22% on the abnormally

thick RPEDC map for AMD eyes (Fig 7D) suggests that 0.22×269≈59 eyes have an abnormally thick RPEDC at that location on the map. Figure 7D also shows that an abnormally thick RPEDC was more likely near the fovea. As expected, abnormalities in the TR thickening maps (Fig 7A, C) were less likely than in the RPEDC thickening maps (Fig 7B, D), making them inefficient metrics for distinguishing between control and AMD eyes.

For completeness, Figure 8 shows the mean NSR thickness for control and AMD eyes. However, because NSR measurements are linearly dependent on the RPEDC and TR data, we did not use the NSR for classification purposes in this article.

Using Thickness Maps to Distinguish Subjects with Age-Related Macular Degeneration from Control Subjects

We used the 5 noted classification methods to distinguish AMD eyes from control eyes. Figure 9 compares the AUC for these classification methods as a function of the analysis cylinder radius centered at the fovea (Fig 9A) and their corresponding ROC curves at the most efficient radius (Fig 9B). More specifically, the best AUC was 0.6843 for method 1 (using TR volume), 0.7801 for method 2 (using RPEDC volume), 0.9856 for method 3 (using the abnormal RPEDC thickness score), 0.9861 for method 4 (using abnormal RPEDC thickness and thinness scores), and 0.9917 for method 5 (using TR and RPEDC volumes plus abnormal RPEDC thickness and thinness scores). For methods 1 to 5, these AUC values were achieved when their corresponding prediction vectors were estimated from data limited to 4-mm, 1.4-mm, 2.4-mm, 2.1-mm, and 2.4-mm radius cylinders centered at the fovea, respectively.

Discussion

Analyzing the topographic distribution of normal and abnormal RPEDC and TR thicknesses across a large atlas of eyes allowed us to identify and validate quantitative biomarkers capable of distinguishing AMD from control eyes with a high accuracy. The best AUCs were achieved by the methods that used the abnormal RPEDC scores (methods 3–5). The model with the best performance used all imaging biomarkers (method 5); however, the abnormal RPEDC thickness score (method 3) was the single most discriminative biomarker of intermediate AMD (Fig 9).

We did not assess imaging biomarker combinations other than the 5 methods described, because method 5 achieved nearly optimal classification based on this dataset. To support this conclusion, we note that 2 of the 269 subjects with AMD had an abnormal RPEDC thickness and thinness scores of zero, whereas RPEDC abnormalities were occasionally present in control eyes. We reviewed SD-OCT images from these subjects and noted only slight abnormalities in their RPEDC thicknesses (Fig 10A, B, available at http://aaojournal.org). In contrast, Figure 10C (available at http://aaojournal.org) shows an even more prominent RPEDC abnormality found in a control subject without macular drusen detected on color fundus photographs. These findings exemplify the main limitation of this study, in which the gold standard for classifying subjects into control and AMD eyes was determined by fundus examination and color fundus photography, despite its known shortcomings.[3] To avoid biasing results in favor of our proposed methodology, subjects misclassified by the gold standard method were not excluded from the study. Fortunately, such cases were rare (Fig 7A, B, E, F).

Quantitative biometry of the macula, RPE, and drusen represents a paradigm shift in the diagnosis and classification of nonadvanced AMD. For more than a decade, the AREDS classification system of color photographs has been the gold standard for AMD grading and risk stratification.[28] However, the classification of intermediate and advanced AMD and

treatment algorithms for neovascular advanced AMD are being revisited with SD-OCT imaging,[21,29] and several recent studies have described confounding errors with color photograph classification of intermediate AMD.[3,21] We recently described how presumed hyperpigmented RPE changes and hypopigmented atrophic changes actually have multiple causes detected by SD-OCT that include intraretinal RPE migration, hyper-reflective drusen cores, small cuticular drusen, subretinal fibrosis, and focal RPE atrophy.[30] More relevant to this report, we previously showed an improvement in the delineation of soft drusen size with SD-OCT over conventional color photography.[3] The advantages of SD-OCT have been further validated by elegant studies of drusen morphology[31] and drusen volume analysis.[32–34]

Our validation of the novel RPEDC segmentation method presents several improvements over previous studies of volumetric drusen analysis. We have tried to overcome several limitations of measuring drusen thickness that were presented by Yehoshua et al.[33] We measure drusen volume from the RPE-photoreceptor interface to the RPE floor, corresponding to the inner border of Bruch's membrane. This method captures pathology such as sub-retinal drusenoid deposits that may be missed by other drusen-specific methods.[33] We did not implement a threshold for ignoring RPEDC thickness less than 10 pixels thick. Although designed to reduce spurious noise, these thresholds ignore small formations such as basal laminar drusen, underestimate the cumulative drusen volume in the region of interest, and fail to accurately capture volume loss due to GA. We analyzed the RPEDC and TR volumes within a 5-mm diameter ring, rather than the AREDS standardized 6-mm diameter, to avoid the confounding influence of non–AMD-related parapapillary atrophy on our cumulative volume measurements.

This validation report is based on subjects in a prospective observational study with standardized follow-up and a control arm of age-matched healthy eyes. Unlike previous studies, our study design enables direct biometric comparisons of AMD and control eyes in the largest atlas published to date.

Analysis of the RPEDC and retinal thickness in normal and AMD eyes resulted in some unexpected observations. It is interesting to note that the maximum RPEDC thickness for control eyes changed as a function of distance from the fovea and was thickest at 0.5 mm distance from the fovea (Fig 5). However, the observation that an abnormally thick RPEDC was found mostly near the fovea for AMD eyes (Fig 5) is supported by previous studies.[35]

It is intriguing to note that the NSR is thicker in AMD versus control eyes at distances greater than 1.175 mm from the fovea (Fig 8D). This finding might seem to differ with previous reports on photoreceptor layer thinning over drusen in non-neovascular AMD eyes using SD-OCT[4] or histopathology.[36] This could be explained by the fact that the NSR includes all neurosensory layers and not just the photoreceptor layer and that these volumes extend beyond the apex of drusen material. Our future studies will evaluate the thicknesses of retinal layers relative to the underlying RPE.

More puzzling is the contrast of our results with the report of Wood et al[37] that retinal thickness, from the ILM to the center of the most posterior hyper-reflective line (RPE), is reduced in the early AMD eyes compared with a control group at multiple locations within 2.0 mm of the fovea. This does not match our report on NSR thickness, which finds AMD and control eyes statistically similar in locations within 1.175 mm of the fovea and NSR thicker in locations beyond 1.175 mm of the fovea in AMD eyes. Indeed, there is a slight difference between definitions of the corresponding layers. Retinal thickness in the article by Wood et al[37] extends to the middle of the RPE layer, whereas in our study it extends to the inner aspect of RPEDC. The similarities or differences in exact level of AMD between these

studies are unclear, because Wood et al[37] described the eyes as having early AMD, yet included eyes with pigmentary change and large drusen. The difference in retinal thickness between these 2 studies may point to the limitations of the current broad categories used to classify AMD on the basis of color fundus imaging. The remaining comparison studies used smaller samples of 16 to 17 patients[4,37] with a slight difference between the mean ages of the participants across studies. A limitation of our study is that although the control eyes are of an elderly population, the mean age of the controls was 8 years less than that of the subjects with AMD. This could affect the retinal and RPE thicknesses, especially because Bruch's membrane thickness has been reported to increase with age.[38] However, we expect that such an impact would be limited because the age-related Bruch's membrane thickness difference in elderly subjects (60–80 years) is less pronounced and is on the order of a few microns,[38] whereas our reported RPEDC/ TR thickness differences between control and AMD eyes is on the order of tens of microns (Fig 5).

We have made the entire dataset for this study freely available online at http://people.duke.edu/wsf59/RPEDC_Ophth_2013_dataset.htm (accessed July 4, 2013) to facilitate future studies by other groups. Included are all 38 800 SD-OCT images of control and AMD eyes, the associated layer boundary segmentations, the RPEDC and TR thickness maps for all eyes, the subject ages, the browsing software, and the statistical analysis. Such information can be used for many other related AMD studies or for evaluating the efficacy of current and future automated image processing algorithms,[22,39,40] and can also be leveraged by researchers without access to such a large pool of patient data. The control patient dataset can also serve as the normative baseline for comparative studies of other ocular and neurologic diseases.[41]

Previous studies report statistically significant differences in the thicknesses of retinal layers measured on SD-OCT systems from different manufacturers.[42,43] To make our results globally applicable across different SD-OCT brands, we have conducted experiments using a model eye (Proceedings of SPIE 7550, Ophthalmic Technologies XX, 75502F, 2010). Our preliminary results indicate differences in measured thickness between and even within manufacturers (e.g., a correction factor of 0.862 would be used to convert our reported thicknesses at central fovea to those from Spectralis [Heidelberg Inc, Heidelberg, Germany]). We will report a detailed analysis in an upcoming publication.

In conclusion, we have established efficient quantitative imaging biomarkers for intermediate AMD as seen on SDOCT. These objective metrics can distinguish diseased from control subjects with 99% precision. In our upcoming publications, we will analyze follow-up images from the same subjects. The utility of RPEDC and TR volume as a predictor of disease progression, or as a clinical trial end point, remains unclear. Changes in drusen, as viewed on color fundus photographs, that led eyes to progress from level 2 to 3 AMD were not found to be correlated with visual acuity preservation in AREDS.[44] Although thickness and volume measurements are currently not a surrogate for disease progression or vision loss in AMD, upcoming studies will determine whether the reported biomarkers can also be used as predictive measures for the progression of intermediate AMD.

Supplementary Material

Refer to Web version on PubMed Central for supplementary material.

Acknowledgments

Funding:

This project was funded in part by the American Health Assistance Foundation, Genentech Grant IST-4400S, and National Institutes of Health Grants R01-EY022691 and P30-EY-005722. The AREDS2 Ancillary SD-OCT Study (ClinicalTrials.gov identifier: NCT00734487) was funded by the Genentech Grant IST-4400S, with clinical imaging equipment support from Bioptigen and a startup donation from Alcon Laboratories. The sponsor or funding organization had no role in the design or conduct of this research.

References

1. Bressler NM. Age-related macular degeneration is the leading cause of blindness. JAMA. 2004; 291:1900–1. [PubMed: 15108691]
2. Khanifar AA, Koreishi AF, Izatt JA, Toth CA. Drusen ultra-structure imaging with spectral domain optical coherence tomography in age-related macular degeneration. Ophthalmology. 2008; 115:1883–90. [PubMed: 18722666]
3. Jain N, Farsiu S, Khanifar AA, et al. Quantitative comparison of drusen segmented on SD-OCT versus drusen delineated on color fundus photographs. Invest Ophthalmol Vis Sci. 2010; 51:4875–83. [PubMed: 20393117]
4. Schuman SG, Koreishi AF, Farsiu S, et al. Photoreceptor layer thinning over drusen in eyes with age-related macular degeneration imaged in vivo with spectral-domain optical coherence tomography. Ophthalmology. 2009; 116:488–96. [PubMed: 19167082]
5. Age-Related Eye Disease Study Research Group. A simplified severity scale for age-related macular degeneration: AREDS report no. 18. Arch Ophthalmol. 2005; 123:1570–4. [PubMed: 16286620]
6. van Leeuwen R, Klaver CC, Vingerling JR, et al. The risk and natural course of age-related maculopathy: follow-up at 6 1/2 years in the Rotterdam Study. Arch Ophthalmol. 2003; 121:519–26. [PubMed: 12695249]
7. Klein R, Klein BE, Tomany SC, et al. Ten-year incidence and progression of age-related maculopathy: the Beaver Dam Eye Study. Ophthalmology. 2002; 109:1767–79. [PubMed: 12359593]
8. Wang J, Foran S, Smith W, Mitchell P. Risk of age-related macular degeneration in eyes with macular drusen or hyper-pigmentation: the Blue Mountains Eye Study cohort. Arch Ophthalmol. 2003; 121:658–63. [PubMed: 12742843]
9. Hageman GS, Luthert PJ, Victor Chong NH, et al. An integrated hypothesis that considers drusen as biomarkers of immune-mediated processes at the RPE-Bruch's membrane interface in aging and age-related macular degeneration. Prog Retin Eye Res. 2001; 20:705–32. [PubMed: 11587915]
10. Pauleikhoff D, Barondes MJ, Minassian D, et al. Drusen as risk factors in age-related macular disease. Am J Ophthalmol. 1990; 109:38–43. [PubMed: 1688685]
11. Yehoshua Z, Rosenfeld PJ, Gregori G, et al. Progression of geographic atrophy in age-related macular degeneration imaged with spectral domain optical coherence tomography. Ophthalmology. 2011; 118:679–86. [PubMed: 21035861]
12. Bearelly S, Chau FY, Koreishi A, et al. Spectral domain optical coherence tomography imaging of geographic atrophy margins. Ophthalmology. 2009; 116:1762–9. [PubMed: 19643488]
13. Burke TR, Rhee DW, Smith RT, et al. Quantification of peripapillary sparing and macular involvement in Stargardt disease (STGD1). Invest Ophthalmol Vis Sci. 2011; 52:8006–15. [PubMed: 21873672]
14. Hood DC, Lin CE, Lazow MA, et al. Thickness of receptor and post-receptor retinal layers in patients with retinitis pigmentosa measured with frequency-domain optical coherence tomography. Invest Ophthalmol Vis Sci. 2009; 50:2328–36. [PubMed: 19011017]
15. Curcio CA, Messinger JD, Sloan KR, et al. Human chorio-retinal layer thicknesses measured in macula-wide, high-resolution histologic sections. Invest Ophthalmol Vis Sci. 2011; 52:3943–54. [PubMed: 21421869]
16. Pappuru RR, Ouyang Y, Nittala MG, et al. Relationship between outer retinal thickness substructures and visual acuity in eyes with dry age-related macular degeneration. Invest Ophthalmol Vis Sci. 2011; 52:6743–8. [PubMed: 21685337]
17. Lee BR, Bartsch DU, Kozak I, et al. Comparison of a novel confocal scanning laser ophthalmoscopy algorithm with optical coherence tomography in measurement of macular thickness and volume. Retina. 2009; 29:1328–34. [PubMed: 19934823]

18. Sadda SR, Stoller G, Boyer DS, et al. Anatomical benefit from ranibizumab treatment of predominantly classic neovascular age-related macular degeneration in the 2-year ANCHOR Study. Retina. 2010; 30:1390–9. [PubMed: 20924261]
19. CATT Research Group. Ranibizumab and bevacizumab for neovascular age-related macular degeneration. N Engl J Med. 2011; 364:1897–908. [PubMed: 21526923]
20. AREDS2 Research Group. Chew EY, Clemons T, SanGiovanni JP, et al. The Age-Related Eye Disease Study 2 (AREDS2): study design and baseline characteristics (AREDS2 report number 1). Ophthalmology. 2012; 119:2282–9. [PubMed: 22840421]
21. Leuschen JN, Schuman SG, Winter KP, et al. Spectral-domain optical coherence tomography characteristics of intermediate age-related macular degeneration. Ophthalmology. 2013; 120:140–50. [PubMed: 22968145]
22. Chiu SJ, Izatt JA, O'Connell RV, et al. Validated automatic segmentation of AMD pathology including drusen and geographic atrophy in SD-OCT images. Invest Ophthalmol Vis Sci. 2012; 53:53–61. [PubMed: 22039246]
23. Chiu SJ, Li XT, Nicholas P, et al. Automatic segmentation of seven retinal layers in SDOCT images congruent with expert manual segmentation. Opt Express. 2010; 18:19413–28. [serial online] Available at: http://www.opticsinfobase.org/oe/abstract.cfm?uri1/4oe-18-18-19413. [PubMed: 20940837]
24. Dobson, AJ. An Introduction to Generalized Linear Models. Chapman & Hall; New York: 1990. p. 21-236.
25. Hastie, TJ.; Tibshirani, RJ.; Friedman, JH. The Elements of Statistical Learning: Data Mining, Inference, and Prediction. 2nd ed.. Springer; New York: 2008. p. 241-8.
26. Kay, SM. Detection Theory. Vol. 2. Prentice-Hall; Upper Saddle River, NJ: 1998. Fundamentals of Statistical Signal Processing.; p. 74-5.
27. Metz CE. Receiver operating characteristic analysis: a tool for the quantitative evaluation of observer performance and imaging systems. J Am Coll Radiol. 2006; 3:413–22. [PubMed: 17412096]
28. Age-Related Eye Disease Study Research Group. The Age-Related Eye Disease Study system for classifying age-related macular degeneration from stereoscopic color fundus photographs: the Age-Related Eye Disease Study report number 6. Am J Ophthalmol. 2001; 132:668–81. [PubMed: 11704028]
29. Freund KB, Zweifel SA, Engelbert M. Do we need a new classification for choroidal neovascularization in age-related macular degeneration? Retina. 2010; 30:1333–49. [PubMed: 20924258]
30. Folgar FA, Chow JH, Farsiu S, et al. Spatial correlation between hyperpigmentary changes on color fundus photography and hyperreflective foci on SDOCT in intermediate AMD. Invest Ophthalmol Vis Sci. 2012; 53:4626–33. [PubMed: 22589439]
31. Spaide RF, Curcio CA. Drusen characterization with multi-modal imaging. Retina. 2010; 30:1441–54. [PubMed: 20924263]
32. Freeman SR, Kozak I, Cheng L, et al. Optical coherence tomography-raster scanning and manual segmentation in determining drusen volume in age-related macular degeneration. Retina. 2010; 30:431–5. [PubMed: 19952989]
33. Yehoshua Z, Wang F, Rosenfeld PJ, et al. Natural history of drusen morphology in age-related macular degeneration using spectral domain optical coherence tomography. Ophthalmology. 2011; 118:2434–41. [PubMed: 21724264]
34. Hartmann KI, Gomez ML, Bartsch DU, et al. Effect of change in drusen evolution on photoreceptor inner segment/outer segment junction. Retina. 2012; 32:1492–9. [PubMed: 22481478]
35. Abdelsalam A, Del Priore L, Zarbin MA. Drusen in age-related macular degeneration: pathogenesis, natural course, and laser photocoagulationeinduced regression. Surv Ophthalmol. 1999; 44:1–29. [PubMed: 10466585]
36. Curcio CA, Medeiros NE, Millican CL. Photoreceptor loss in age-related macular degeneration. Invest Ophthalmol Vis Sci. 1996; 37:1236–49. [PubMed: 8641827]

37. Wood A, Binns A, Margrain T, et al. Retinal and choroidal thickness in early age-related macular degeneration. Am J Ophthalmol. 2011; 152:1030–8. [PubMed: 21851922]

38. Okubo A, Rosa RH, Bunce CV, et al. The relationships of age changes in retinal pigment epithelium and Bruch's membrane. Invest Ophthalmol Vis Sci. 1999; 40:443–9. [PubMed: 9950604]

39. Leng T, Rosenfeld PJ, Gregori G, et al. Spectral domain optical coherence tomography characteristics of cuticular drusen. Retina. 2009; 29:988–93. [PubMed: 19584657]

40. Gregori G, Wang F, Rosenfeld PJ, et al. Spectral domain optical coherence tomography imaging of drusen in nonexudative age-related macular degeneration. Ophthalmology. 2011; 118:1373–9. [PubMed: 21388687]

41. Tátrai E, Simó M, Iljicsov A, et al. In vivo evaluation of retinal neurodegeneration in patients with multiple sclerosis. PLoS ONE. 2012; 7:e30922. [serial online] Available at: http://www.plosone.org/article/info%3Adoi%2F10.1371%2Fjournal.pone.0030922. [PubMed: 22292076]

42. de Kinkelder R, de Bruin DM, Verbraak FD, et al. Comparison of retinal nerve fiber layer thickness measurements by spectral-domain optical coherence tomography systems using a phantom eye model. J Biophotonics. 2012; 6:314–20. [PubMed: 22810965]

43. Lin P, Mettu PS, Pomerleau DL, et al. Image inversion on spectral-domain optical coherence tomography optimizes choroidal thickness measurement and visualization of outer choroidal detail through improved outer choroidal contrast. Invest Ophthalmol Vis Sci. 2012; 53:1874–82. [PubMed: 22410550]

44. Age-Related Eye Disease Study Research Group. A randomized, placebo-controlled, clinical trial of high-dose supplementation with vitamins C and E, beta carotene, and zinc for age-related macular degeneration and vision loss: AREDS report no. 8. Arch Ophthalmol. 2001; 119:1417–36. [PubMed: 11594942]

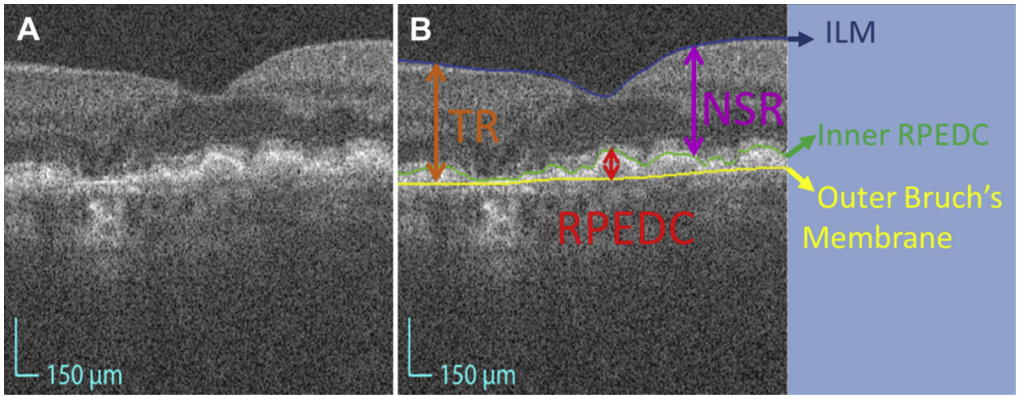

Figure 1.

Definition of the target segmented layers and layer boundaries. **A**, Magnified foveal spectral-domain optical coherence tomography (SD-OCT) image with 6.70 μm lateral resolution and 3.24 μm axial resolution. **B**, Delineation of the target layer boundaries: the inner aspect of the inner limiting membrane (ILM) in blue, the inner aspect of the retinal pigment epithelium drusen complex (RPEDC) in green, and the outer aspect of Bruch's membrane in yellow. **A** and **B**, These boundaries isolate the total retina (TR) (*orange arrow* from blue to yellow), neurosensory retinal (NSR) (*purple arrow* from blue to green), and RPEDC (*red arrow* from green to yellow).

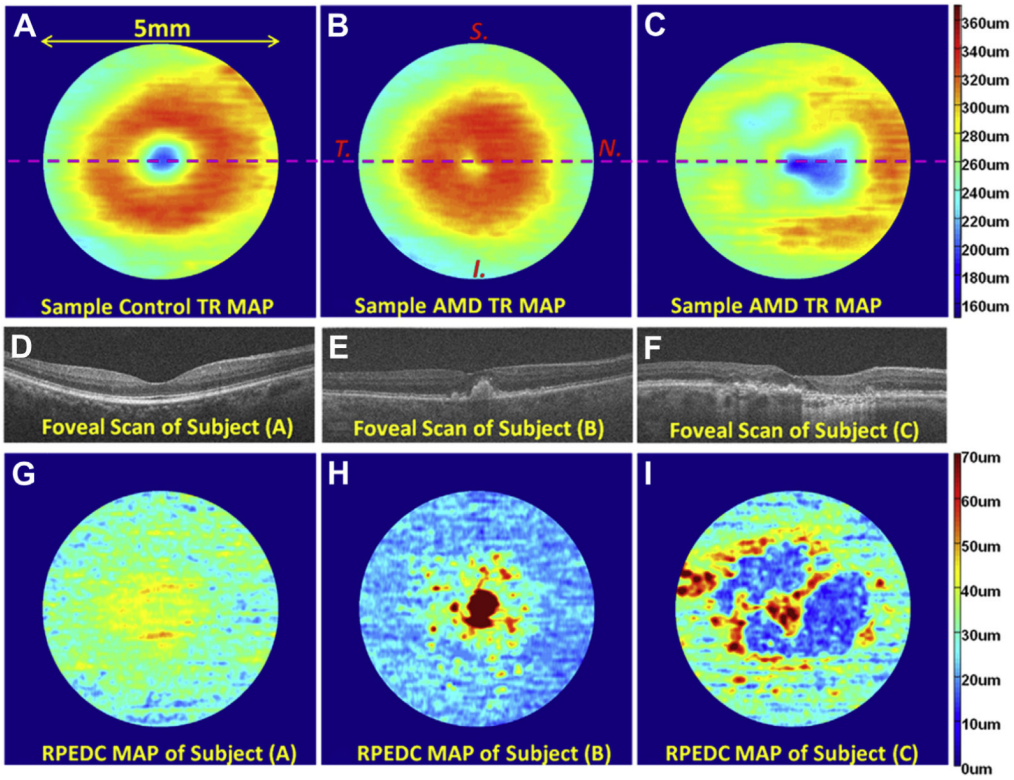

Figure 2.

Example total retina (TR) and retinal pigment epithelium drusen complex (RPEDC) thickness maps created from control and non-neovascular age-related macular degeneration (AMD) eyes. **A**, TR map of a control subject centered at the fovea. The location of the foveal spectral-domain optical coherence tomography (SD-OCT) scan is annotated by the purple line. **B**, TR map of a subjects with AMD annotated with the superior, nasal, inferior, and temporal directions. All thickness maps in this article have this same orientation. **C**, TR of another subject with AMD. **D** and **E**, Foveal scans of the maps in (**A–C**), respectively. **G**, RPEDC thickness map of the normal subject in (A). **H**, RPEDC thickness map of the subject with AMD in (B). Thickening around the fovea (*red regions*) is indicative of drusen. **I**, RPEDC thickness map of the subject with AMD in (C). Thickening around the fovea (*yellow regions*) is representative of drusen, whereas thinning (*blue regions*) is representative of geographic atrophy (GA).

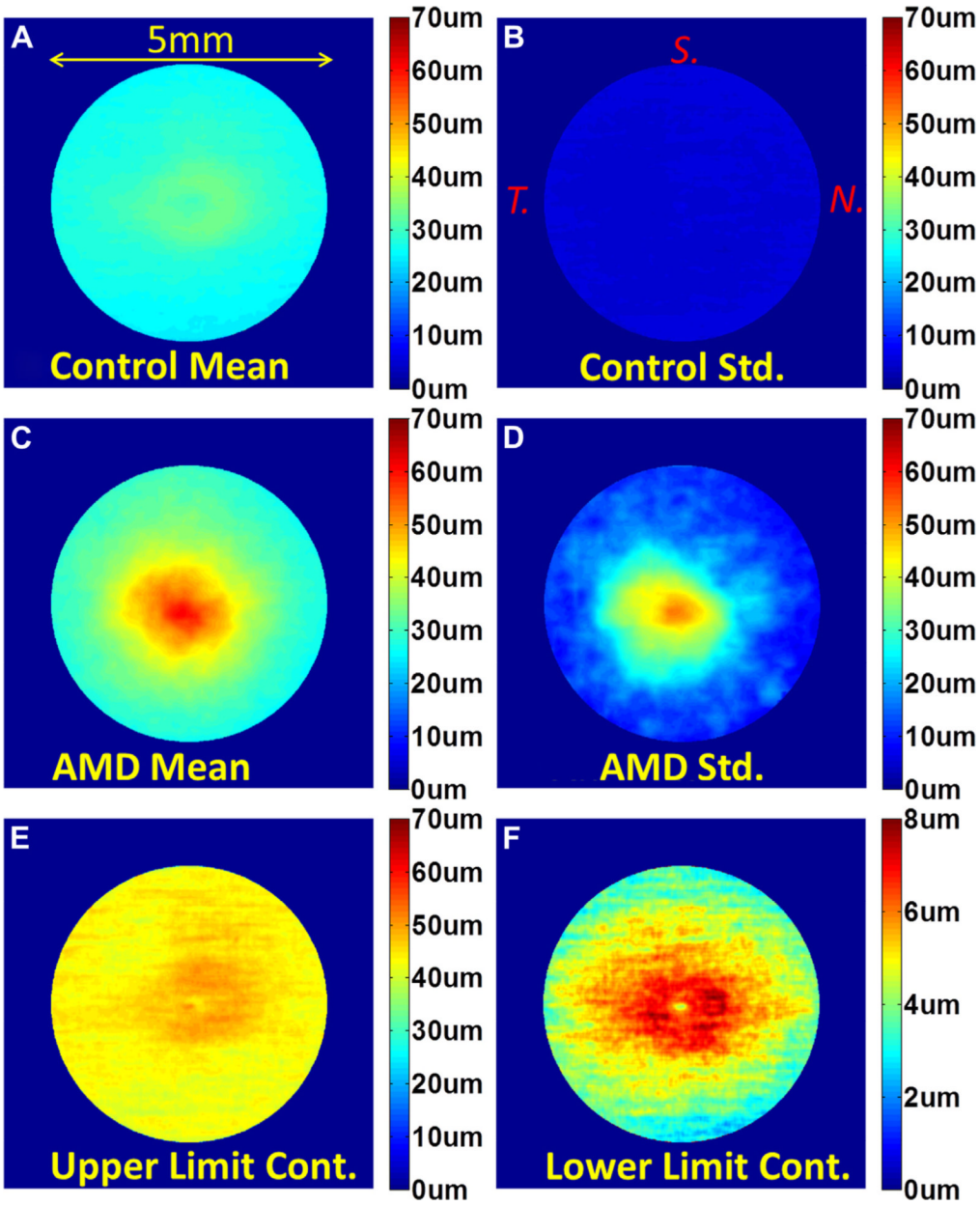

Figure 3.

Statistical analysis of retinal pigment epithelium drusen complex (RPEDC) thickness maps centered at the fovea. **A**, Mean RPEDC thickness map for 115 control subjects. **B**, Standard deviation RPEDC thickness map for 115 control subjects. **C**, Mean RPEDC thickness map for 269 subjects with age-related macular degeneration (AMD). **D**, Standard deviation RPEDC thickness map for 269 subjects with AMD. **E**, Upper-limit RPEDC thickness map (Fig 4A + 3 × Fig 4B) for control subjects (i.e., within 3 standard deviations) used to detect drusenoid regions. **F**, Lower-limit RPEDC thickness map (Fig 4A – 3 × Fig 4B) for control subjects (within 3 standard deviations of) used to detect geographic atrophy (GA) regions. N = nasal; S = superior; T = temporal.

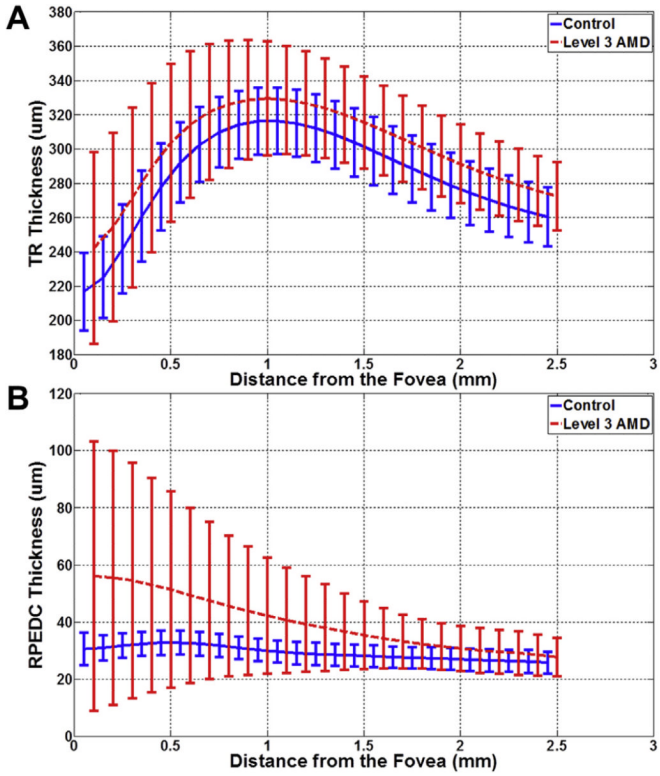

Figure 5.

Average retinal pigment epithelium drusen complex (RPEDC) (**A**) and total retina (TR) (**B**) thicknesses as a function of the distance from the fovea for control subjects (*blue*) and subjects with intermediate age-related macular degeneration (AMD) (*red*). The error bars represent 1 standard deviation. The differences in TR and RPEDC thicknesses in control and intermediate AMD eyes were statistically significant for all measurement points.

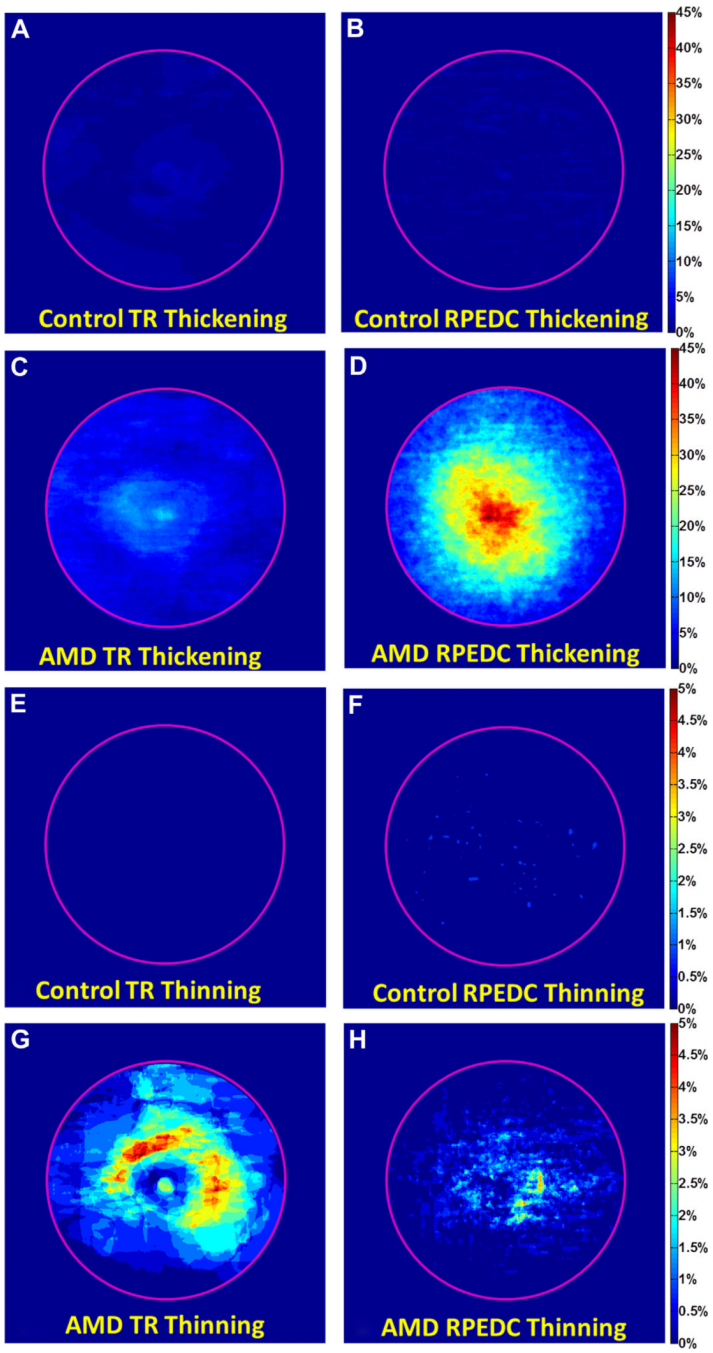

Figure 7.

Probability maps for abnormal total retina (TR) and retinal pigment epithelium drusen complex (RPEDC) thickening (**A–D**) and abnormal TR and RPEDC thinning (**E–H**) in age-related macular degeneration (AMD) and normal eyes. For example, a probability of 1% in (**B**) suggests that 0.01×115≈1 control eye has an abnormally thick RPEDC, whereas a probability of 22% in (**D**) suggests that 0.22×269≈59 AMD eyes have an abnormally thick RPEDC.

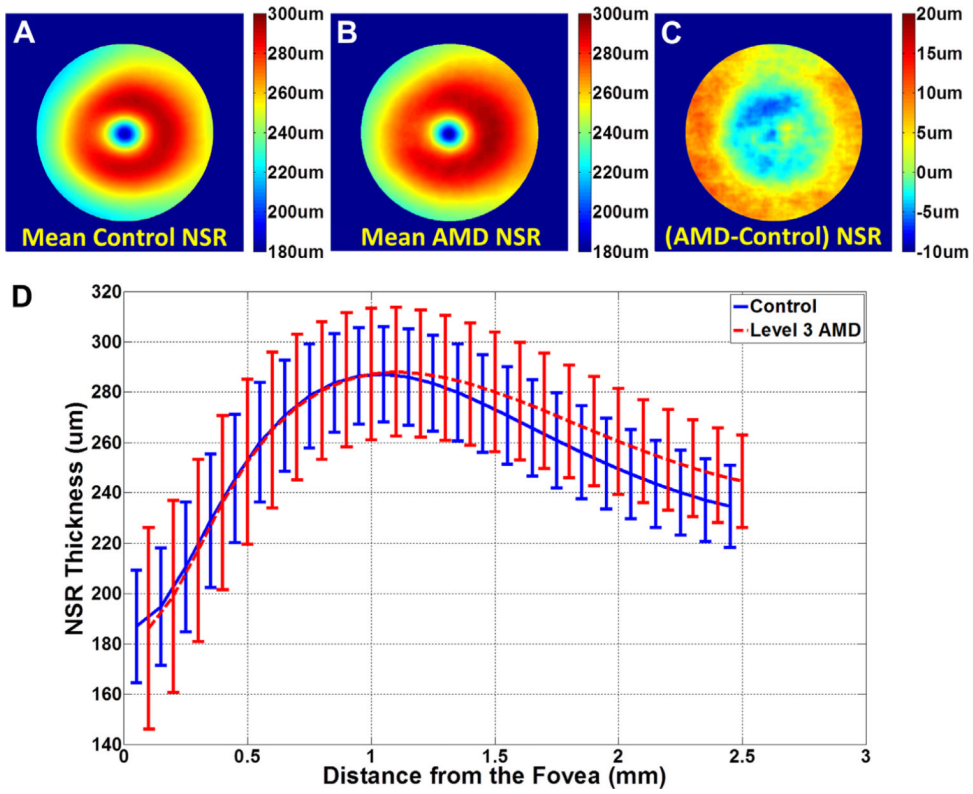

Figure 8.

Mean neurosensory retinal (NSR) thickness maps for (**A**) 115 control subjects and (**B**) 269 subjects with age-related macular degeneration (AMD). The maps are centered at the fovea and 5 mm in diameter. **C**, Thickness map showing the mean AMD NSR map (**B**) subtracted by the mean control NSR map (**A**). The NSR is significantly thicker in AMD versus control eyes at distances >1 mm from the fovea. **D**, Average NSR thicknesses as a function of the distance from the fovea for control subjects (*blue*) and subjects with intermediate AMD (*red*). Error bars represent 1 standard deviation. In contrast to previous reports,[37] the differences in NSR thicknesses in control and intermediate AMD eyes were only statistically significant (Wilcoxon rank-sum test, $P < 0.05$) for measurement points beyond 0.175 mm from the fovea.

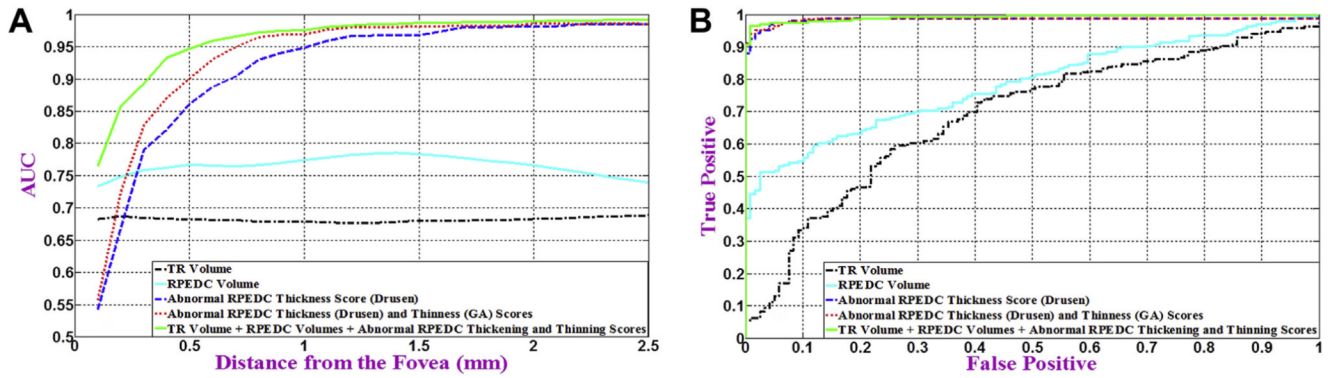

Figure 9.

Distinguishing age-related macular degeneration (AMD) from control eyes using 5 different imaging biomarkers. **A**, Variation of the area under the curve (AUC) of receiver operating characteristic (ROC) per radius of analysis centered at the fovea for each method. **B**, The ROC curve at the best radius from (**A**) for each method. Method 1: the total retina (TR) volume (*black dashed-dotted curve*, AUC = 0.6843), method 2: the retinal pigment epithelium drusen complex (RPEDC) volume (*cyan solid curve*, AUC = 0.7801), method 3: abnormal RPEDC thickness score (*dashed-dotted blue curve*, AUC = 0.9856), method 4: abnormal RPEDC thickness and thinness scores (*red dotted curve*, AUC = 0.9861), and method 5: all 4 markers, including the TR and RPEDC volumes plus the abnormal RPEDC thickening and thinning scores (*solid green curve*, AUC = 0.9917).